24AM1E-07

Complex-Source Beam Diffraction by a Wedge: Exact and Complex Rays Solutions

Michael Katsav [#1], Ehud Heyman [#2], Ludger Klinkenbusch [*3]

[#] *School of Electrical Engineering, Tel Aviv University, Tel Aviv 69978, Israel*
[1] katsav.michael@gmail.com [2] heyman@tau.ac.il

[*] *Institute of Electrical and Information Engineering, Christian-Albrechts-Universität zu Kiel Kaiserstr. 2, D-24143 Kiel, Germany*
[3] lbk@tf.uni-kiel.de

***Abstract*—Complex-source beam diffraction by a wedge is explored as a function of the beam direction and displacement from the edge. The complex ray solution is derived and compares to exact solutions via the the complex multipole expansion and via the Sommerfeld integral.**

I. Introduction

The complex-source beam (CSB) provides a canonical setting for rigorous study of beam diffraction phenomena as well as of various solution techniques [1], [2]. In the present work we explore the field of a 2D CSB scattering by a wedge as a function of the beam direction and displacement from the edge. We derive an asymptotic solution via complex ray tracing (CRT) [3] and complex-ray GTD [4], and also calculate the exact solution via the the complex multipole expansion and via the Sommerfeld integral. It is interesting to note that the corresponding 3D problem for a short-pulse excitation has a closed form solution [5]. The present work extends the analysis in [6] where we only considered the complex multipole solution for a CSB hitting exactly *at* the edge. The latter result were extended to 3D cone diffraction problem in [7]. The long term goal of this research is the derivation of scattering and diffraction coefficients for a beam impinging on a tip of a cone, as a function of the beam parameters: the collimation, direction and the displacement from the tip. The principles of our approach are demonstrated here in the context of the 2D case.

II. Physical Layout

Referring to Fig. 1, we consider an acoustically soft wedge whose faces are at $\phi = 0$ and $\phi = \varphi$. The incident beam is modeled by as radiation from a point-source located at the complex coordinate point

$$\mathbf{r}_c = \mathbf{R}_0 + i\mathbf{b} \tag{1}$$

where $\mathbf{R}_0 = (R_0, \phi_0)$ and $\mathbf{b} = (b, \phi_b)$ are real vectors expressed here in polar form. It can be shown that in the real coordinates space, the field generated by source is a CSB beam that emerge from the real point $\mathbf{R}_0$ in the direction of $\mathbf{b}$ (Fig. 1). $\mathbf{R}_0$ is the center of the beam waist, while $b = |\mathbf{b}|$ is the beam collimation length (Rayleigh length), and ϕ_b is the beam direction. Henceforth we denote $\phi_b = \pi + \phi_0 + \delta_b$, so that δ_b represents the beam displacement from the edge. A time-harmonic dependence $e^{-i\omega t}$ is assumed and suppressed throughout.

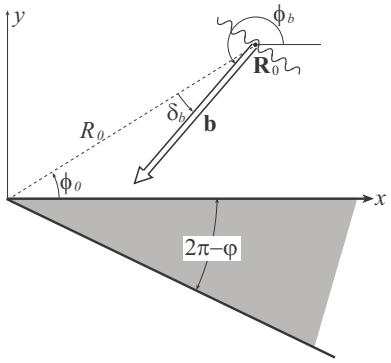

Fig. 1. CSB and wedge geometry. The double arrow schematizes the CSB emerging from the source disk [2] which is centered at $\mathbf{R}_0$. The small angle δ_b defines the beam displacement from the edge.

The Cartesian coordinates of the complex source-point are

$$x_c = R_0 \cos\phi_0 + ib\cos\phi_b \tag{2a}$$
$$y_c = R_0 \sin\phi_0 + ib\sin\phi_b \tag{2b}$$

where substituting $\phi_b = \pi + \phi_0 + \delta_b$ and assuming $\delta_b \ll 1$ we obtain the first order approximation

$$x_c \approx (R_0 - ib)\cos\phi_0 + ib\delta_b \sin\phi_0 \tag{3a}$$
$$y_c \approx (R_0 - ib)\sin\phi_0 - ib\delta_b \cos\phi_0 \tag{3b}$$

If the beam hits near the edge ($\delta_b \ll 1$) one finds from (3) to first order in δ_b that $r_c = R_0 - ib$ and $\phi_c = \phi_0 - ib\delta_b/(R_0 - ib)$.

III. 2D Multipole Expansion

The exact solution of the field may be expressed in terms of the multipole expansion representation of the complex source Green's function for a soft (Dirichlet) wedge [8, Eq. 6.5.12]

$$\psi(\mathbf{r}) = \frac{i\pi}{\varphi}\sum_{\ell=1}^{\infty} J_{\nu_\ell}(kr_<)H^{(1)}_{\nu_\ell}(kr_>)\sin(\nu_\ell\phi)\sin(\nu_\ell\phi_c) \tag{4}$$

where (r_c, ϕ_c) are the complex source polar coordinates in (2), $\nu_\ell = \ell\pi/\varphi$, $(r_<, r_>) = (r_c, r)$ or (r, r_c) if $\Re\{r_c\} \lessgtr r$, respectively, J_n and $H_n^{(1)}$ are Bessel functions and Hankel functions of the 1st kind, respectively, and $k = \omega/c$ is the wavenumber. Note that the convergence of the multipole series depend on the magnitude of the argument of the Bessel functions.

IV. 2D Sommerfeld Integral Solution

The spectral integral solution for the 2D Green's function in the presence of a perfectly conducting wedge is derived in [8], Secs. 6.3a and 6.5a and 6.5c. Here we present the extension of this integral to the complex source case, obtaining from [8, Eq. 6.3.5]

$$\psi(\mathbf{r}) = \frac{-1}{8\pi}\int_{-i\infty}^{i\infty} dw\, H_0^{(1)}(k\chi)A(\phi,\phi_c;w) + \psi^{\text{CRT}}(\mathbf{r}), \quad (5)$$

where $\chi = \sqrt{r^2 + r_c^2 + 2rr_c\cos w}$ and ψ^{CRT} is the complex ray field (see Sec. V-A). A is defined in general in [8], Eq. 6.3.6. For the Dirichlet boundary conditions it is given in several alternative forms in Eqs. 6.5.4–6.5.9 there (see also discussions in [9, Eqs. (3)–(4)] and [5, Eqs. (13)]). Specifically, we use here $-2A(\phi,\phi_c;w) \to D(\phi - w, \phi_c)$ where

$$D(\phi - w, \phi_c) = \frac{-(2\pi/\varphi)\sin(\pi^2/\varphi)}{\cos(\pi(\phi - w - \phi_c)/\varphi) - \cos(\pi^2/\varphi)} - \frac{-(2\pi/\varphi)\sin(\pi^2/\varphi)}{\cos(\pi(\phi - w + \phi_c)/\varphi) - \cos(\pi^2/\varphi)} \quad (6)$$

This form reduces to the diffraction coefficient in (9).

In order to understand the Sommerfeld integral (5) and to perform it properly, on needs to understand the behavior of the complex poles in D. For simplicity, let us assume in (1) that $\phi_0 < \pi$. The relevant poles of the first and second terms in (6) are given then by $w_{1,2} = \phi \mp \phi_c - \pi$. It follows that if the observation point is located in the "shadow" zone of the complex direct rays in Sec. V-A(1) or of the complex reflected rays in Sec. V-A(2), then $w_{1,2}$ are located, respectively, on the right hand side of the imaginary w axis. Thus, the integration contour in (5) should be taken such that w_1 is located on its left or right hand side for points in the "lit" or "shadow" zones of the direct complex rays, respectively, and likewise w_2 is located on its left or right hand side for points in the "lit" or "shadow" zones of the reflected complex rays, respectively. The residue contributions of $w_{1,2}$ as they cross the integration contour from left to right cancel exactly the direct and reflected ray contributions in ψ^{CRT} of (5).

Note that by extracting the complex ray field ψ^{CRT} explicitly, the Sommerfeld integral in (5) may be regarded as the "diffracted field" associated with the complex ray field. Actually, it provides a uniform representation to the non-uniform complex ray diffraction in (9).

V. Complex Ray Tracing and Complex Ray GTD

We start by extending the two faces of the wedge to the complex coordinate domain. Face 1 is described by $(x, y) = (\xi_1, 0)$ where ξ_1 is a complex coordinate. Likewise, face 2 is described by $(x, y) = (\xi_2\cos\varphi, \xi_2\sin\varphi)$ where ξ_2 is also complex. The two planes intersect at the origin where $\xi_{1,2} = 0$, which defines the edge of the wedge. We therefore define faces 1 and 2 of the wedge by adding the conditions $\Re\{\xi_{1,2}\} > 0$.

For calculation purposes it is convenient to introduce planes $1, 2$ as the planar extensions of faces $1, 2$. These planes are defined by the relations above but without the restriction on $\Re\{\xi_{1,2}\}$.

A. Complex Rays

Following [3], a complex ray that emerges from a complex point $\mathbf{r}_0$ is defined by

$$\mathbf{r}(s) = \mathbf{r}_0 + s\mathring{\mathbf{s}} \quad (7)$$

where $\mathring{\mathbf{s}} = (\mathring{s}_x, \mathring{s}_y)$ is the complex ray direction such that $\mathring{s}_x^2 + \mathring{s}_y^2 = 1$, and s is the complex $distance$ parameter along the ray. The positive ray direction is defined by the direction of increasing $\Re\{s\}$. Henceforth, a complex unite vector is defined by an over-ring.

1) The Field of the Direct Ray From $\mathbf{r}'$ to the Real Point $\mathbf{r}$

We start by calculating the direct ray from the complex source point $\mathbf{r}_c$ to a given real observation point $\mathbf{r} = (x, y)$. The distance along the ray is defined by $s(\mathbf{r}) = \sqrt{(x - x_c)^2 + (y - y_c)^2}$ with $\Re\{s\} > 0$. The properties of this distance function has been explored thoroughly in the literature (see e.g., in [2, Fig. 2a and Sec. 2.A]). It has been demonstrated that when substituting this s into the free-space Green's yields a beam-field that propagates in real space along the direction of the vector $\mathbf{b}$.

Next, for that $\mathbf{r}$ we also calculate the ray direction $\mathring{\boldsymbol{s}}(\mathbf{r})$. Using (7), we now find $\mathbf{q}_j$, the complex point where this ray intercepts plane j defined above, and s_{qj}, the distance along the ray from $\mathbf{r}_c$ to $\mathbf{q}_j$. Note, the s_{qj} is defined uniquely via (7) and it does not involve a square root. Therefor, $\Re\{s_{qj}\}$ may be positive, if the complex ray that emerges from $\mathbf{r}_c$ intercepts plane j, or negative, if the complex ray is intercepts plane j and then converges onto $\mathbf{r}_c$.

Selection rule 1: This ray is included in the field representation if $\mathbf{q}_j$ does not belong to the complex extension of face j, or if it does belong to the complex extension of face j but with $\Re\{s_{qj}\} < 0$. The field of that ray is given by

$$\psi^i(\mathbf{r}) = G(\mathbf{r}, \mathbf{r}_c) = \frac{i}{4}H_0^{(1)}(ks(\mathbf{r})) \sim \frac{e^{iks(\mathbf{r})+i\pi/4}}{\sqrt{8\pi ks(\mathbf{r})}} \quad (8)$$

where the last term is the conventional approximation for $|ks| \gg 1$. Expression (8) describes the incident CSB fields.

2) The field of the Reflected Rays

In order to calculate the reflected complex rays it is convenient to consider the image points $\bar{\mathbf{r}}_{cj}$ of $\mathbf{r}_c$ with respect to plane j. Next we calculate rays R_j from $\bar{\mathbf{r}}_{cj}$ to $\mathbf{r}$ in the same manner we have done it before, obtaining also $\bar{s}_j$ with $\Re\{\bar{s}_j\} > 0$ and $\mathring{\bar{\boldsymbol{s}}}_j$. We also calculate the complex points $\bar{\mathbf{q}}_j$

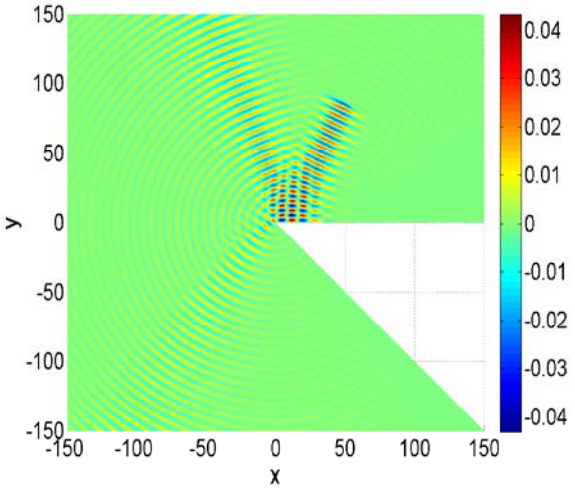

Fig. 2. Exact field calculation via (4) of the CSB field diffracted by a 45° wedge for $kR_0 = 100$, $\phi_0 = \pi/3$, $kb = 80$, $\delta_b = 5^\circ$. The figure depicts the real part of the total field.

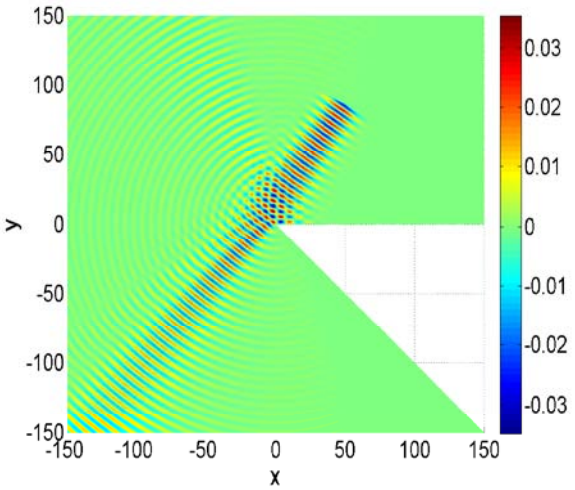

Fig. 3. As in Fig. 2 but for $\delta_b = -5^\circ$.

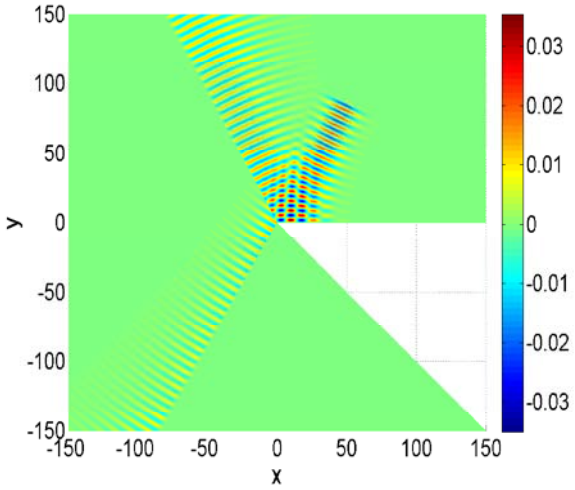

Fig. 4. As in Fig. 2 but using only CRT analysis and without complex ray diffraction.

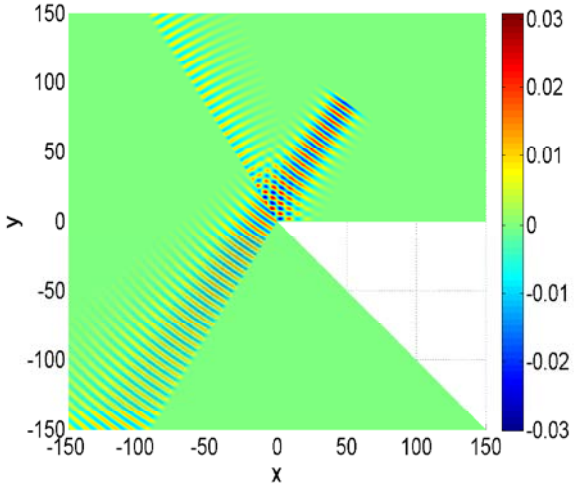

Fig. 5. As in Fig. 4 but for the configuration in Fig. 3.

where these rays intercept plane j and $\bar{s}_{qj}$, the distances from $\mathbf{r}_c$ to $\mathbf{q}_j$. These rays correspond to the rays going from $\mathbf{r}_c$ to $\mathbf{r}$ after reflection at $\mathbf{q}_j$ on the complex plane j.

Selection rule 2: R_j is included in the field representation only if $\mathbf{r}_{qj}$ belongs to the complex extension of face j and $\Re\{\bar{s}_j\} > \Re\{\bar{s}_{qj}\}$. The reflected field ψ^r is given by the expression in (8) with $s \to \bar{s}_j$ and with the boundary reflection coefficient.

B. Complex Ray Diffraction

As noted earlier, the complex edge is at the real point $(x, y) = \mathbf{0}$. Therefore the diffracted field is given by

$$\psi^d(\mathbf{r}) = G(\mathbf{0}, \mathbf{r}_c) G(\mathbf{r}, \mathbf{0}) D(\phi, \phi_c), \tag{9}$$

where D is given in (6) with $w = 0$. Actually (9) is the saddle point contribution of (5) obtained by replacing $H_0^{(1)}(k\chi) = \sqrt{\frac{2}{\pi k \chi}} e^{ik\chi - i\pi/4}$. One finds that $\chi' = -rr_c \sin(w)/\chi$ hence the saddle point is at $w = 0$. The result in (9) is obtained by noting that $\chi(0) = r + r_c$ and $\chi''(0) = -rr_c/(r + r_c)$.

The asymptotic saddle point contribution in (9) is valid only if the stationary point $w = 0$ is sufficiently isolated from the poles of D in (6). As noted there, the relevant poles of the first and second terms in (6) are given by $w_{1,2} = \phi \mp \phi_c - \pi$, respectively. If the beam hits very close to the edge ($\delta_b \ll 1$), then $\phi_c \sim \phi_0$ (see discussion after (3)). In that case $w_{1,2}$ are near $w = 0$ in the shadow and reflection transition zones $\phi \approx \pm\phi_0 + \pi$ so that (9) is no longer valid and should be replaced by a uniform asymptotic evaluation of the integral in (5). Further away from these zones, the poles are sufficiently removed from $w = 0$ and the non-uniform complex ray diffraction contribution in (9) applies well (see Figs. 6 and 7). If, on the other hand, the beam hits far from the edge, then $\phi_c \nsim \phi_0$ (see (3)) so that $w_{1,2}$ never pass near the stationary

point and (9) is valid uniformly for all ϕ.

VI. Numerical Results

We consider the diffraction of a CSB field by a 45° wedge (i.e., $\varphi = 3\pi/2$). The beam parameters are $\mathbf{R}_0 = (R_0, \phi_0) = (100, 60^\circ)$, $b = 80$ where the units are set such that $k = 1$. The resulting fields for beam displacements $\delta_b = \pm 5^\circ$ (see Fig .1) are shown in Figs. 2 and 3, respectively. These results were calculated using the multipole expansion in (4). The scattered and diffracted fields are clearly identified.

Figs. 4 and 5 depict the CRT fields corresponding to the configurations in Figs. 2 and 3, respectively. Note the in view of the selection rules in Secs. V-A(1) and (2) for the direct and reflected fields, these fields are discontinuous in the shadow and reflections boundaries.

Finally, Figs. 6 and 7 depict the fields in the configurations of Figs. 2 and 3, respectively, as a function of ϕ at a distance $kr = 200$. The calculations via the exact multipole expansion (4) and the exact Sommerfeld integral (5) (red and black dashed lines, respectively) are indistinguishable on the figure scale. Also shown are the asymptotic CRT field without and with the diffraction (blue-dashed and green-dotted lines, respectively). Far from the transition zones, the CRT with diffraction provides a faithful representation of the field, but this formulation fails in the transition where a uniform representation for the diffraction coefficient is required, as discussed after (6) and (9). However, as discussed there, if the beam hits sufficiently for from the edge then the non-uniform diffraction coefficient of (9) does provide a uniform representation for all ϕ.

VII. Conclusion

We explored the field of a 2D CSB scattering by a wedge as a function of the beam direction and displacement from the edge. We presented a new exact solution via the the complex multipole expansion (4) and compared it with the Sommerfeld integral solution (5). The latter has been formulated in a way that extracts explicitly the asymptotic complex ray field ψ^{CRT}. The properties of the the Sommerfeld integral solution depend on the lit and shadow zones generated by the wedge. Consequently, we explored the complex ray tracing (CRT) for the wedge geometry and the *selection rules* that delineate these lit and shadow zones. The validity of the new exact formulations were demonstrated via numerical calculations (Figs. 6, 7) that have also demonstrated the intriguing physical features of the field (see Figs. 2, 3). Further insight have been provided by the CRT solution (Figs. 4, 5). The long term goal of this research is the derivation of scattering and diffraction coefficients for a beam impinging on a tip of a cone [7].

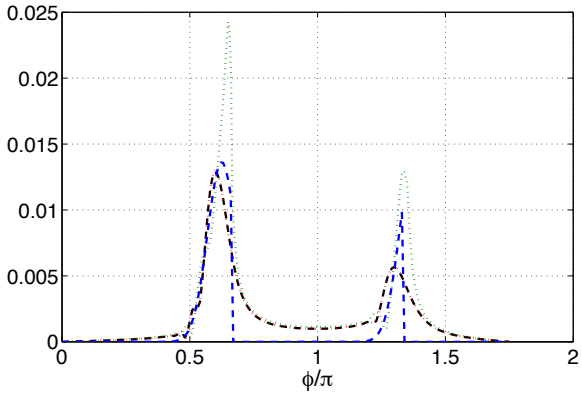

Fig. 6. The field corresponding to the configurations in Fig. 2 as a function of ϕ at a distance $kr = 200$. The figure compares the exact fields calculated via the multipole expansion (4) (black) and via the Sommerfeld integral (5) (red) to the asymptotic CRT field (blue) and the CRT plus diffraction (green).

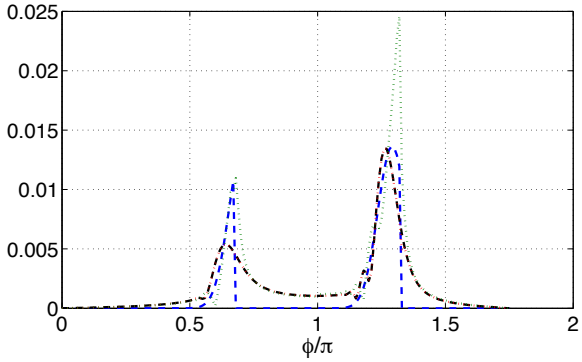

Fig. 7. As in Fig. 6, but for the problem configuration of Fig. 3 with $\delta_b = -5^\circ$.

Acknowledgment

M. Katsav and E. Heyman would like to acknowledge partial support by the Israeli Science Foundation, Grant No. 263/11. L. Klinkenbusch would like to acknowledge partial support by the Deutsche Forschungsgemeinschaft (DFG), Grant No. KL 815/10-2.

References

[1] L.B. Felsen, "Complex-source-point solutions of the field equations and their relation to the propagation and scattering of Gaussian beams," in *Symposia Matematica, Istituto Nazionale di Alta Matematica, Vol. XVIII*, 40–56, Academic Press, London, 1976.

[2] E. Heyman and L.B. Felsen, "Gaussian beam and pulsed beam dynamics: Complex source and spectrum formulations within and beyond paraxial asymptotics," *J. Opt. Soc. Am. A*, vol. 18, pp. 1588–1611, 2001.

[3] Y.D. Wang and G.A. Deschamps, "Application of complex ray tracing to scattering problems," *Proceedings of the IEEE*, vol. 62(11), pp. 1541–1551, 1974.

[4] G.A. Suedan and E.V. Jull, "Beam diffraction by planar and parabolic reflectors" *IEEE Trans. Antennas Propagat.* vol. 39(4), 521–527, 1991.

[5] R. Ianconescu and E. Heyman, "Pulsed-beam diffraction by a perfectly conducting wedge: Exact solution", *IEEE Trans. Antennas and Propagat.*, vol. 42(10), pp. 1377–1385, 1994.CRT with the diffraction

[6] M. Katsav, E. Heyman, and L. Klinkenbusch, "Scattering and diffraction of a Complex-Source Beam by a wedge," in Proc. Joint IEEE AP-S and URSI Symposium, July 2012, Chicago, IL, USA, paper 358.10.

[7] M. Katsav, E. Heyman, and L. Klinkenbusch, "Complex -source beam diffraction by an acoustically soft or hard circular cone," in *Proc. the Int. Conf. on Electromagnetics in Advanced Applications (ICEAA),* Sept. 2012, Cape Town, South Africa.

[8] L.Felsen, N.Marcuvitz, *Radiation and Scattering of waves*, Prentice-Hall, New Jersey, 1973.

[9] R. Ianconescu and E. Heyman, "Pulsed field diffraction by a perfectly conducting wedge: A spectral theory of transient (STT) analysis," *IEEE Trans. Antennas Propagat.*, vol. 42(6), pp. 781–789, 1994.